JAM CM Journal of Applied Mathematics and Computational Mechanics 2022, 21(2), 39-50
www.amcm.pcz.pl p-ISSN 2299-9965
DOI: 10.17512/jamcm.2022.2.04 e-ISSN 2353-0588

APPLICATION OF A NEAR WALL MODEL TO NAVIER-STOKES EQUATIONS WITH NONLINEAR TIME-RELAXATION MODEL

Özgül İlhan

Department of Mathematics, Faculty of Science, Muğla Sıtkı Koçman University
Muğla, Turkey
oilhan@mu.edu.tr

Received: 1 December 2021; Accepted: 21 May 2022

Abstract. It is difficult and essential to determine appropriate boundary conditions for the flow averages because they depend on the behavior of the unknown flow near the wall. Large-eddy simulation (LES) is one of the promising approaches. LES estimates local spatial averages $\overline{u}$ of the velocity u of the fluid. The main problem is modeling near-wall turbulence in complex geometries. Inspired by the works of Navier and Maxwell, the boundary conditions are developed on the wall. In this study, the appropriate friction coefficient for 2-D laminar flows is computed, and existing boundary layer theories are used to improve numerical boundary conditions for flow averages. The slip with friction and penetration with resistance boundary conditions are considered. Numerical tests on two-dimensional channel flow across a step using this boundary condition on the top and bottom wall and the step are performed.

MSC 2010: *76-06, 76F40, 76F65, 76D05, 76D10*
Keywords: *boundary layers, laminar, near wall models (NWM), Navier-Stokes equation with nonlinear time-relaxation model (NSE-NTR)*

1. Introduction

Large-eddy simulation (LES) is one of the valuable approximations for dynamic features of the flow. LES estimates local, spatial flow averages above a prespecified length scale δ. Predicting the behavior of turbulent flows is a common phenomenon in engineering. Turbulence arising from a flow and a wall interaction is an essential model in Large-eddy simulations (LES). This interaction is usually seen in complex geometries. Thus, the difficulties arising from LES in engineering applications cause to find appropriate boundary conditions for flow averages. Flow averages (with constant averaging radius δ) are not naturally local, and these flow averages behave like unknown, primary turbulence flow near the boundary. The problem of finding boundary conditions with a constant averaging radius δ is called Near Wall Modeling in LES. This boundary condition is also known as Near Wall Model (NWM) [1]. We consider this problem in this study.

The flow over a backward-facing step is a fundamental benchmark problem as it occurs in many applications in engineering. These engineering applications include the flows around the buildings, inside combustors, industrial ducts, and cooling of electronic devices. In these phenomena, separation, recirculation, and reattachment are essential in transporting momentum in the flow. Separation, recirculation, and reattachment can be explained with this example. Inside an expanding duct, recirculation influences the recovery of the flow downstream from the expansion. From this event, it can be concluded that the separation of the boundary layer from the surface occurs by a reverse pressure gradient. This gradient causes the formation of a mixing layer that attaches to the surfaces. The flow over a backward-facing step is an example of the geometry of these events.

The NWM model was firstly studied by Deardoff [2] in LES. A nonlocal condition on the wall shear stress was firstly used by Schumann [3]. These NWMs are nonlocal. Thus, LES models are challenging to solve with these boundary conditions. However, they can be examined as containing a normal derivative of the wall stress against a complex condition since this imposes higher-order boundary conditions than the equations do. (Therefore, there are many chances for mathematical understanding of existing NWMs.)

There are different approaches to NWM. Recently, Bose has applied a dynamic slip boundary condition to wall-bounded large-eddy simulation [4]. Also, Bostrom has studied boundary conditions for spectral simulations of atmospheric boundary layers [5]. Shafiq et al. investigated the stagnation point flow of Walters-B fluid induced by a Riga plate [6]. Recently, Cao studied barotropic compressible Navier--Stokes equations with Navier-type boundary conditions in a two-dimensional simply connected bounded domain [7]. Winter analyzed a novel weak imposition of the general Navier boundary condition, provided methods to counteract geometrical approximation errors, and showed the applicability of the method within a wetting flow context [8]. Finally, new near-wall models were investigated by Fakhari, Posa and Balaras [9, 10]. Numerous numerical tests have been studied on turbulence models [11]. Hill considered the α-models of turbulence; these models have minor differences. In this study, a near-wall model for the Navier-Stokes equation with a nonlinear time-relaxation model (NSE-NTR) in the light of the [12–16] is improved. The aim is to improve a physical NWM suitable for laminar channel flows.

We consider the following NSE-NTR model [17],

$$u_t + u\cdot\nabla u - \nu\Delta u + \nabla p + \kappa|u-\overline{u}|(u-\overline{u}) = f, \text{ in } \Omega$$
$$\nabla\cdot u = 0 \text{ in } \Omega, \quad u = h \text{ on } \partial(\Omega), \quad u(x,0) = u_0(x).$$

It must be found $u \in V = (H_0^1(\Omega))^2 = \{v \in (H^1(\Omega))^2 : v|_{\partial(\Omega)} = 0\}$ and $p \in P = L_0(\Omega) = \{L^2(\Omega) : \int_\Omega p dx = 0\}$. When the NSE-NTR model is discretized in time

using Backward Euler; it can be written as follows

$$\begin{aligned}&(\frac{u^h_{n+1}-u^h_n}{\Delta t},v^h)+b^*(u^h_{n+1},u^h_{n+1},v^h)+\nu(\nabla u^h_{n+1},\nabla v^h)\\&-(p^h_{n+1},\nabla v^h)+(\kappa|u^h_n-\overline{u}^h_n|(u^h_{n+1}-\overline{u}^h_{n+1}),v^h)=(f_{n+1},v^h)\\&(\nabla\cdot u^{n+1},q)=0,\quad \forall q\in P.\end{aligned}\tag{1}$$

where (.,.) denotes the L^2 inner product, $v^h\in V$ is a test function and $b^*(a,b,c)=$ $=\frac{1}{2}(a\cdot\nabla b,c)-\frac{1}{2}(a\cdot\nabla c,b)$ and

$$\begin{aligned}&\frac{\overline{u}^h_{n+1}-\overline{u}^h_n}{\Delta t}=\frac{|u^h_n-\overline{u}^h_n|(u^h_{n+1}-\overline{u}^h_{n+1})}{\delta}\\&\overline{u}^h_0=u^h_0\end{aligned}\tag{2}$$

where u^h_{n+1} is the only unknown at each step. u^h_{n+1} can be found easily using (2). u^h_n is the velocity solution of the previous time step, and v^h is test function, the time step is $\Delta t=0.01$. This means that one second corresponds to 100 iterations. The Box filter is given by

$$g(x)=\left\{\begin{array}{ll}1, & \text{if all } |x_j|<\frac{1}{2}\\0, & otherwise\end{array}\right\}\tag{3}$$

where $1\le j\le d$. There are many other filters, $g(x)$, see, e.g. [18]. When all functions except Ω are zero, the large eddies are given as follows

$$\overline{\mathbf{u}}:=g*\mathbf{u}=\int_{\mathbb{R}^d}g(y-x)u(x)dx,\quad \overline{\mathbf{p}}:=g*p,\quad \bar{\mathbf{f}}:=g*f$$

The most used boundary condition is $\overline{u}=0$ on Ω. Using the example of the behavior of hurricanes and tornadoes [14,15] and the work of Navier [19] and Maxwell [20], the equations of NWMs can be written as follows

$$\overline{\mathbf{u}}\cdot\mathbf{n}=0 \text{ and } \beta\overline{\mathbf{u}}\cdot\ \tau_i+2Re^{-1}\mathbf{n}\cdot D(\overline{\mathbf{u}})\cdot\ \tau_i=0 \text{ on } \partial(\Omega)\tag{4}$$

where $\mathbf{n}$ is outward unit normal, $\{\tau_1,\tau_2,...\tau_{d-1}\}$ is an orthonormal system of tangential vectors and β is the efficient friction coefficient. β must be computed. The boundary condition (4) does not impose equilibrium: time fluctuations of the normal stress at the wall will result through (4) in time fluctuations of the slip velocity. In this study, we present numerical studies of two-dimensional channel flows across a step and show the influence of the friction parameter on the position of the reattachment point.

A mathematical signification of no-penetration and slip with resistance is the boundary condition (4) which is called Navier's slip law [19]. In 1879, Maxwell [20] derived the Navier-Stokes equations from the kinetic theory of gases by use of the

averaging process and corrected the boundary condition (4). In Maxwell's derivation, the friction coefficient β was found as follows,

$$\beta \approx \frac{microscopiclengthscale}{macroscopiclengthscale}.$$

This work proposes that for LES, we should find a friction coefficient β scaling with $\beta \approx Re^{-1}\frac{L}{\delta}$, $L = diam(\Omega)$.

The conditions (4) similar to no-slip conditions as $\delta \to 0$ for fixed Re and to free-slip conditions as $Re \to \infty$ for fixed δ. Therefore, such a scaling is convenient. $\overline{\mathbf{u}}$ on $\partial(\Omega)$ behaves relative to $\mathbf{u}$ near $\partial(\Omega)$. The accuracy of the definition of near wall flows is very important for the used analysis. In section 2, the near wall modeling for 2-D laminar flows is considered. The optimal friction coefficient (9) is computed. Its asymptotic behaviors are given as $\delta \to 0$ for fixed Re and $Re \to \infty$ for fixed δ in Proposition 1. It is examined for a flow over the flat plate (and therefore also over a smoothly curving surface whose curvature is negligible).

In Section 3, numerical tests are presented on a 2-D flow across a step. The boundary condition (4) is applied to NSE-NTR [17] for these tests. These numerical tests show the dependency of the reattachment point of the recirculating vortex on the friction parameter.

In this study, a nonlocal condition (4) is replaced by a local condition (no-slip boundary condition ($u = 0$)) for $\overline{\mathbf{u}}$. There are considerable studies about the well-posedness of nonlocal boundary conditions for the Navier-Stokes equations; thus, this boundary condition must be reduced to a local boundary condition. Besides, to calculate the friction coefficient, we must know u near the walls. Here, the boundary layer theory's accuracy is analyzed. In some cases, the simple boundary layer theory should be changed, and the friction coefficient β should be recalculated. These cases are such that flows against a pressure gradient, geometries for which the curvature κ of $\partial\Omega$ are not negligible, and near stagnation points.

2. Uniform suction in 2-D

In this section, a laminar boundary layer is considered. There are different studies on the laminar and turbulence boundary layer theory; see, e.g., [3]. The friction coefficient can be calculated using other descriptions [14, 16, 21], but it is calculated for the wall law of a laminar boundary layer in this section. Consider the flat plane $\Omega = \{(x,y), y > 0\}$ [14]. The wall law of a laminar boundary layer on a flat plate is as follows [18]

$$u = U_\infty(1 - exp(-|V_0|Rey)), \text{for } y > 0, \quad v = V_0, \quad \text{for } y > 0 \tag{5}$$

where U_∞ is free stream velocity and V_0 is a negative constant.

We want to compute the friction coefficient $\beta(\delta, Re)$ of the boundary layer model (5). For this purpose, let $u = 0$, $v = 0$ on the plane $y < 0$ and $n = (0,-1)$ be the outward pointing normal vector with respect to Ω on $\partial\Omega = y = 0$ and $\tau = (1,0)$ be an orthonormal system of tangential vectors. All velocity components are extended by zero outside Ω. Therefore, using the equations,

$$\overline{u}\cdot n = 0 \text{ and } \beta\overline{u}\tau_i + 2Re^{-1}n\cdot D(\overline{u})\tau_i = 0 \quad \text{on} \quad \partial\Omega$$

the friction coefficient can be calculated following

$$\beta(\delta, Re) = Re^{-1}\frac{\frac{\partial\overline{u}}{\partial y}(x,0)}{\overline{u}(x,0)} \tag{6}$$

At first, using (5) we can calculate $\overline{u}(x,0)$,

$$\begin{aligned}\overline{u}(x,0) = g_{\mathbf{u}}(x,0) &= \int_{-\infty}^{\infty}\int_{0}^{\infty} g(x-x', y-y')u(x',y')dx'dy' \\ &= \int_{-\frac{\delta}{2}}^{\frac{\delta}{2}}\int_{0}^{\frac{\delta}{2}} \frac{U_\infty}{\delta^3}(1-exp(-|V_0|Rey'))dy'dx' = \frac{U_\infty}{2\delta} + \frac{U_\infty}{\delta^2|V_0|Re}(exp(-|V_0|Re\frac{\delta}{2}) - 1)\end{aligned} \tag{7}$$

Also, it can be written,

$$\frac{\partial\overline{u}}{\partial y}(x,0) = g * \frac{\partial u}{\partial y}(x,0) = \int_{-\frac{\delta}{2}}^{\frac{\delta}{2}}\int_{0}^{\frac{\delta}{2}} \frac{U_\infty|V_0|Re}{\delta^3}(exp(-|V_0|Rey'))dy'dx' = -\frac{U_\infty}{\delta^2}(exp(-|V_0|Re\frac{\delta}{2}) + 1) \tag{8}$$

Using (6), (7) and (8), we get the friction coefficient for the laminar boundary layer wall law

$$\beta(\delta, Re) = Re^{-1}\frac{\frac{\partial\overline{u}}{\partial y}(x,0)}{\overline{u}(x,0)} = \frac{1}{Re}\frac{\exp(-\frac{\delta}{2}|V_0|Re) + 1}{\frac{\delta}{2} + \frac{1}{2|V_0|Re}(\exp(-\frac{\delta}{2}|V_0|Re) - 1)} \tag{9}$$

PROPOSITION 1 $\beta(\delta, Re)$ is given in (9). Thus, the following asymptotic results are satisfied.

If Re is constant, so, $\lim_{\delta\to 0}\beta(\delta, Re) = \infty$.

If δ is constant, then $\lim_{Re\to\infty}\beta(\delta, Re) = 0$.

PROOF The proof of limits in Proposition 1 is clear. The asymptotic behaviors are presented in Figure 1.

REMARK 2 The friction law examined in this section is linear and it is not appropriate for recirculating flows. The nonlinear friction laws for recirculating flows has

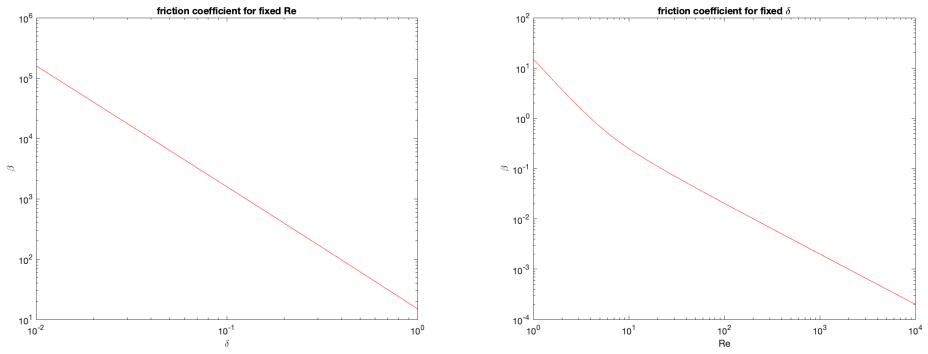

Fig. 1. Behavior of $\beta(\delta, Re)$ with respect to δ and Re, respectively

been studied, see [14, 16]. The formula $\beta = Re^{-1}\dfrac{L}{\delta}$ of Maxwell is satisfied by limits in Proposition 1.

3. A numerical test

In laminar flow simulations, firstly, the eddies form behind the step; afterward, eddies interact with the wall, and finally, the eddies detach from the wall to move towards the channel outlet, and again new eddies form. Hence, the wall model used is important. We conceive a simple, unresolved flow which is a recirculation obtained by flow wall interaction. We present a benchmark problem of two-dimensional channel flow over a backward-facing step. This problem was considered in [11, 14–16, 21]. We investigate the dependency of the position of the reattachment point of the recirculating eddy in two-dimensional channel flow with different values of the friction parameter β.

The domain is a 40×10 channel with a 1×1 step five units into the channel at the bottom (Fig. 2). Flow on the left-hand side of the channel is prescribed as the inflow boundary condition. We present results for a parabolic inflow profile. The parabolic inflow profile is $\mathbf{u} = (u, v)^T$, with $u = \dfrac{y(10-y)}{25}$, $v = 0$. The boundary condition (4) is applied on the top and bottom boundary and also on the step. The aim of the boundary condition (4) is to capture the correct behavior of a flow on a coarser temporal and spatial discretization. On the right side of the channel, the flow leaves the domain, and this flow is an outflow boundary condition. No-slip boundary conditions and boundary conditions (4) are applied to NSE-NTR.

Our aim is to compute the position of the reattachment point of the recirculating vortex behind the step. The end of the step is at the position $x = 6$. The slip with friction boundary condition causes the tangential velocity on the bottom boundary not to be lost. Therefore, the point where the sign of the tangential velocity at the bottom boundary changes is called the reattachment point. The tangential velocity is negative on the left side of the reattachment point and positive on the right.

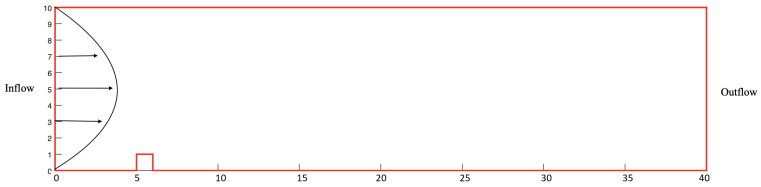

Fig. 2. Domain of two-dimensional channel with a step

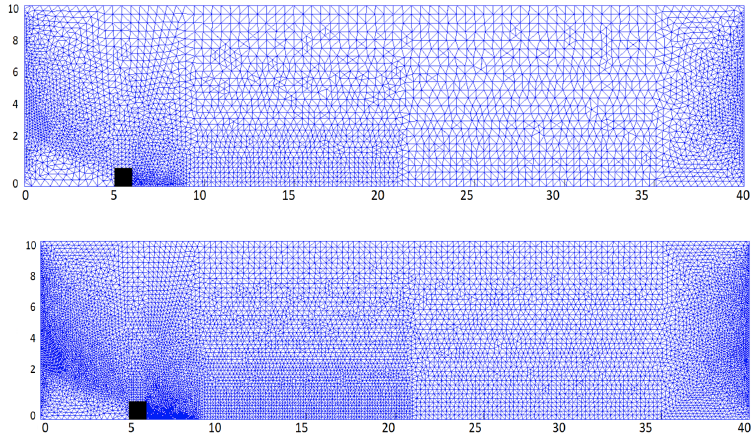

Fig. 3. Two-dimensional channel with a step, coarse mesh (top, (level = 1)) and fine mesh (bottom, (level = 2))

The computations are applied on a coarse and fine grid. These grids are given in Figure 3. The solutions obtained are compared for $Re = 200$ and $Re = 600$ and the friction coefficients $\beta = 0.001$, $\beta = 1$ and $\beta = 10$. FreeFEM++ [22] is used for calculations. The NSE-NTR is discretized in time with the Backward Euler and in space with the Galerkin finite element method.

The coarse mesh requires 33716 and 4305 degrees of freedom for velocity and pressure, respectively, and similarly, the fine mesh needs 85056 and 10777 degrees of freedom for velocity and pressure, respectively. The no-slip boundary condition is implemented in the solution of the NSE-NTR (NSE-NTR+No-Slip), and the

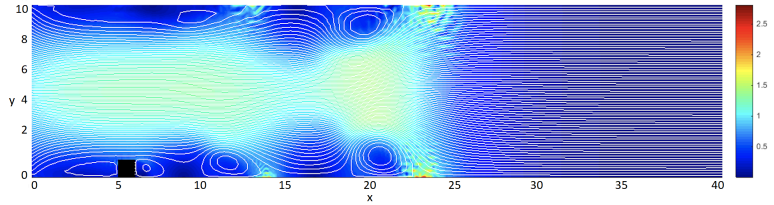

Fig. 4. The streamlines and NSE+NTR+SWF solutions on coarse mesh and at time $T = 40$, for $Re = 200$, $\beta = 0.001$

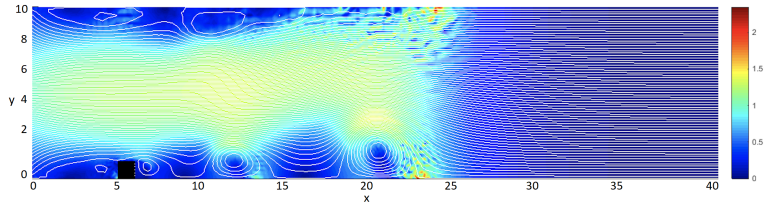

Fig. 5. The streamlines and NSE+NTR+SWF solutions on coarse mesh and at time $T = 40$, for $Re = 600$, $\beta = 1$

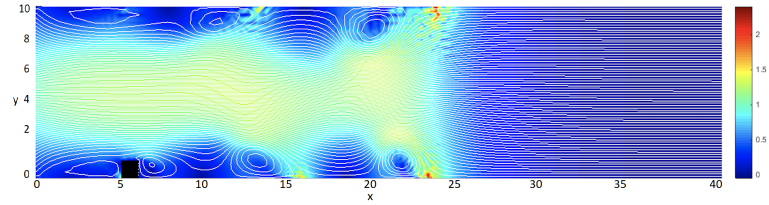

Fig. 6. The streamlines and NSE+NTR+SWF solutions on coarse mesh and at time $T = 40$, for $Re = 200$, $\beta = 10$

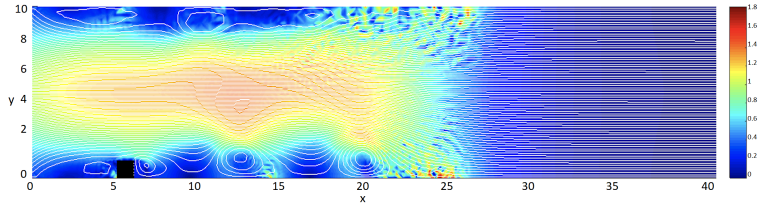

Fig. 7. The streamlines and NSE+NTR+SWF solutions on coarse mesh and at time $T = 40$, for $Re = 600$, $\beta = 10$

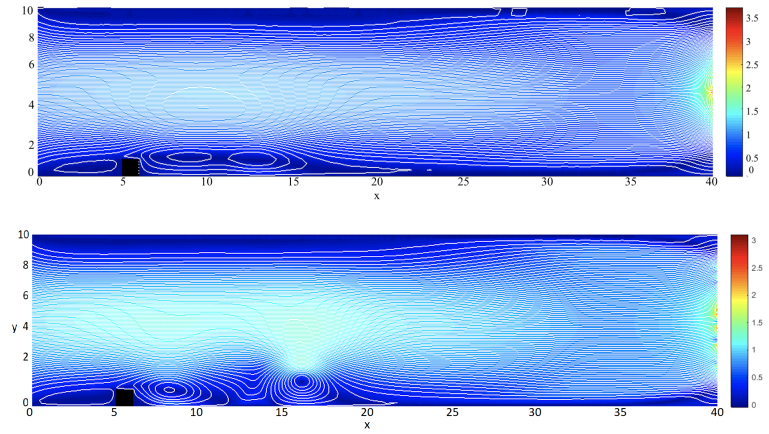

Fig. 8. The streamlines and NSE+NTR+No-Slip solutions on fine mesh and at time $T = 40$, for $Re = 200$ and $Re = 600$, respectively (Reference Solutions)

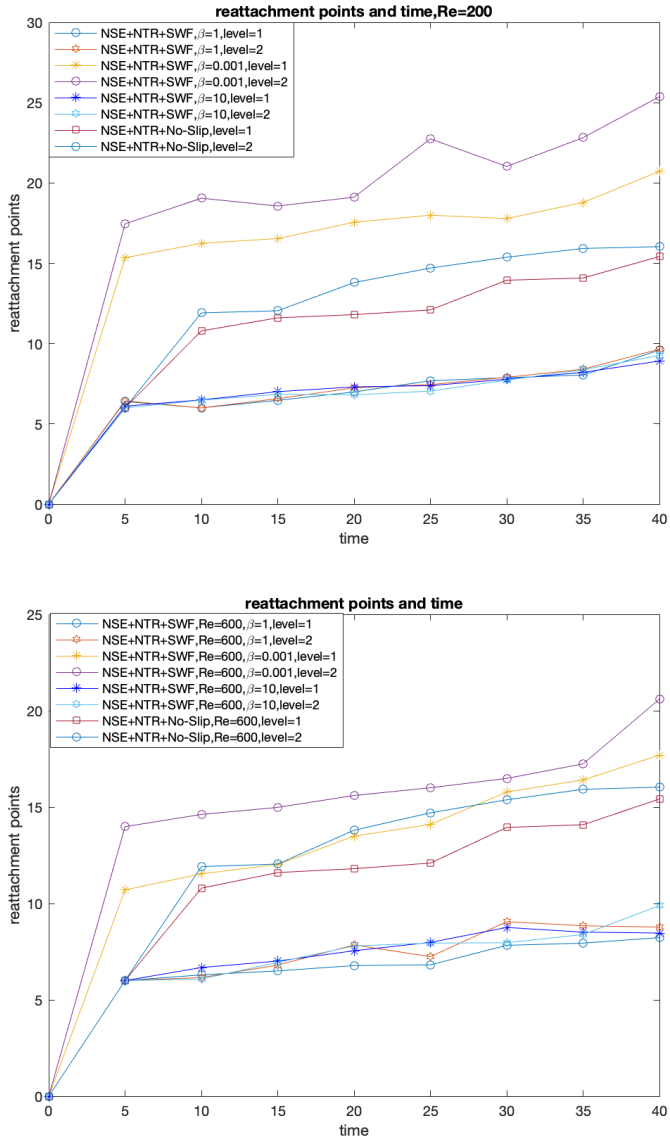

Fig. 9. Time and reattachment points

SWF boundary condition (4) is implemented in the solution of the NSE-NTR (NSE-NTR+SWF). We compared the NSE-NTR+No-Slip solutions, taken as reference solutions and obtained using the fine grid, and NSE-NTR+SWF solutions obtained using a coarse grid. Comparing different cases in under-resolved simulations with a reference solution will make our study valuable. We also compared the solutions of NSE-NTR+SWF for different values of the friction coefficients β.

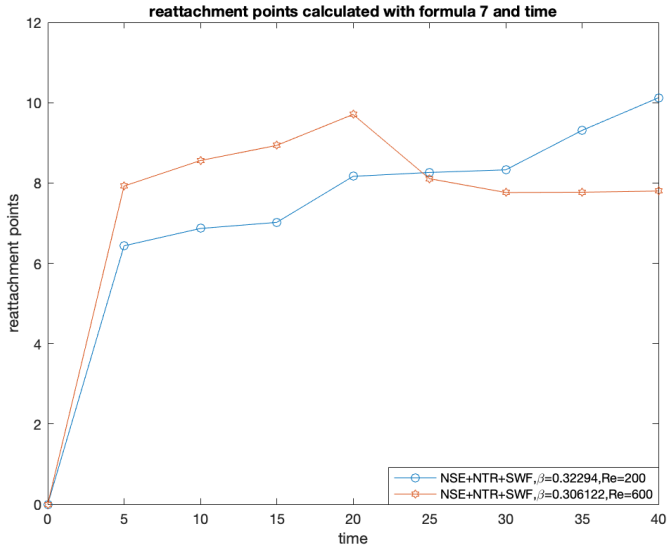

Fig. 10. Time and reattachment points

For $\beta = 0.001, 1$ and 10, we can conclude that the flow is periodic, i.e., eddies are formed behind the step and then shed. This formation is an expected quantitative and qualitative behavior for the given values of β. But, in our numerical tests for all grids, we can see that as the friction coefficient decreases, the reattachment points increase. Similarly, we can observe that as the Reynolds number increases, the reattachment points decrease. These results are given in Figure 9. For $\beta = 0.001$, there are two important changes in the eddy shedding. First, reattachment points move slower, i.e., the eddy is closer to the step. Another change is that the eddies behind the step are larger. This can be seen in Figure 4.

For $\beta = 1$, eddy separates from the bottom boundary at around $x = 20$ and at time $T = 40$ and then moves downstream. This can be observed in Figure 5. Figures 6 and 7 show that for $\beta = 10$, the eddy separates from the bottom boundary at around $x = 25$ and at time $T = 40$ and then moves towards to downstream. Additionally, the eddy is farther from the step. While the SWF boundary condition causes eddy formation at the top boundary, the no-slip boundary condition does not cause eddy formation at the top boundary. We can observe this in all figures. Reattachment points are farther from the step for fine mesh, but they are closer to the step for coarse mesh (Fig. 9). We can say that the eddy is farther from the step for $Re = 200$ and closer to the step for $Re = 600$. The coarse mesh solutions are shown in Figures 4-7. When we compare these solutions with the references solutions, we can say that these solutions can accurately predict the behavior of the eddies behind the step. Moreover, the streamlines are resolved, and there is no oscillation in the streamlines.

The reattachment points computed using the friction coefficient beta calculated with formula (9) are very close to the reattachment points calculated using reference

solutions (Fig. 10). So we can say that the improved NWM is appropriate for the physical flow of fluid.

Figures 4-7 show that NSE-NTR+SWF simulations are improved NSE-NTR+ No-Slip simulations, and the results of simulations are as expected. In addition, NSE-NTR+SWF simulations accurately predict the behavior of the flow behind the step even for coarse meshes.

By an appropriate choice of β on a coarse mesh (level 1), it may not generally be possible to calculate the reattachment point for no-slip boundary conditions on a fine mesh (level 2); see [15]. Therefore, no-slip boundary conditions should always be applied in the standard way with the appropriate degrees of freedom at the boundary. The NSE-NTR+SWF simulations presented in Figures 4-7 (on coarse mesh) capture more reattachment points than the NSE-NTR+No-Slip simulations presented in Figure 8 (on fine mesh). Thus, this reduces the computation time and is the cost of energy.

4. Conclusions

In this study, a NWM is improved for the NSE-NTR model. Box filter and uniform suction are used to calculate the average velocity u in the NWM. An appropriate friction coefficient for 2-D laminar flows is computed and then its asymptotic behaviors are given as $\delta \to 0$ for fixed Re and $Re \to \infty$ for fixed δ. The friction law examined in this study is linear. The Maxwell formula is consistent with the formulas we found. Numerical tests are presented for the 2-D flow of a fluid over a full step with slip with friction boundary conditions and Reynolds numbers 200 and 600, respectively. Results are as expected. For all grids which have been implemented in our numerical tests, as the friction coefficient increases, the reattachment length decreases, and the size of the recirculating vortex also decreases. Besides, as the Reynolds number increases, the reattachment points decrease. Therefore, concerning our study of the NWM, it can be observed that this NWM improves the estimate of the reattachment length in all simulations. Using the NWM presented in this study, the results are close to the reference results. Achieving smooth results on coarse meshes reduces computation time. The improved NWM agrees with the physics of the flow. All simulations are appropriate for a real-world problem. 3-D laminar and turbulent flows can be studied in future works.

References

[1] Berselli, L.C., Iliescu, T., & Layton, W.J. (2006). *Mathematics of Large Eddy Simulation of Turbulent Flows*. Berlin Heidelberg: Springer-Verlag.

[2] Deardoff, J.W. (1970). A numerical study of three-dimensional turbulent channel flow at large Reynolds numbers. *J. Fluid Mech.*, *41*, 453-480.

[3] Schumann, U. (1975). Subgrid scale model for finite difference simulations of turbulent flows in plane channels and annuli. *J. Comput. Phys.*, *18*, 376-404.

[4] Bose, S.T., & Moin, P. (2014). A dynamic slip boundary condition for wall-modeled large-eddy simulation. *Physics of Fluids*, *26*, (015104).

[5] Bostrom, E. (2017). *Boundary Conditions for Spectral Simulations of Atmospheric Boundary Layers*. PhD thesis. Department of Mechanics, Stockholm: Royal Institute of Technology.

[6] Anum Shafiq, A.T., & Hammouch, Z. (2018). Impact of radiation in a stagnation point flow of walters B fluid towards a riga plate. *Thermal Science and Engineering Progress*, *6*, 27-33.

[7] Cao, Y. (2021). *Global classical solutions to the compressible navier-stokes equations with navier-type slip boundary condition in 2d bounded domains*. arXiv:2102.10235v2, April.

[8] Winter, M.E. (2020). *Weak Imposition of the General Navier Condition for Cut Finite Elements with Application to Wetting Processes*, PhD thesis, Fakultat fur Maschinenwesen, Technischen Universitat Munchen.

[9] Fakhari, A. (2019). A new wall model for large eddy simulation of separated flows. *Fluids*, *4*(197), DOI: 10.3390/fluids4040197.

[10] Posa, A., & Balaras, E. (2014). Model-based near-wall reconstructions for immersed-boundary methods. *J. Theor. Comput. Fluid Dyn.*, *28*, 473-483.

[11] Hill, G.R. (2010). *Benchmark Testing the α-models of Turbulence*. Master of Science, the Graduate School of Clemson University.

[12] Galdi G.P., & Layton, W.J. (2000). Approximation of the larger eddies in fluid motion II: A model for space filtered flow. *Math. Models and Meth. In Appl. Science*, *10*(3), 343-350.

[13] Ilhan, O. (2018). *Turbulansli Sinir Tabakasi icin Duvar Kenari Modeli ve Modelin Logaritmik Kanunla Testleri*. PhD thesis. Mugla Sitki Kocman University, Institute of Science.

[14] John, V., Layton, W.J., & Sahin, N., (2004). Derivation and analysis of near wall models for channel and recirculating flows. *Comput. Math. Appl.*, *28*, 1135-1151.

[15] John, V. (2002). Slip with friction and penetration with resistance boundary conditions for the Navier-Stokes equations – numerical tests and aspects of the implementation. *J. Comp. Appl. Math.*, *147*, 287-300.

[16] Sahin, N. (2003). *Derivation, Analysis and Testing of New Near Wall Models for Large Eddy Simulation*. PhD thesis. Department of Mathematics, Pittsburgh University.

[17] Isik, O.R., Yuksel, G., & Demir, B. (2018). Analysis of second order and unconditioanally stable for BDF2-AB2 method for the Navier-Stokes Equations with nonlinear time relaxation. *Numerical Methods for Partial Differential Equations*, *34*(6), 2060-2078.

[18] Pope, S.B. (2000). *Turbulent Flows*. Cambridge University Press.

[19] Navier, C.L.M.H. (1823). Memoire sur les lois du movement des fluiales. *Mem. Acad. Royal Society*, *6*, 389-440.

[20] Maxwell, J.C. (1879). On stresses in rarefied gases arising from inequalities of temperature. *Royal Society Phil. Trans.*, *170*, 249-256.

[21] Ilhan, O., & Sahin, N. (2022). Testing of logarithmic-law for the slip with friction boundary condition. *International Journal of Nonlinear Sciences and Numerical Simulation*, DOI: 10.1515/ijnsns-2021-0184.

[22] Hecht, F., Pironneau, O., & Ohtsuka K. (2022). Freefem++ manual, url=http://www.freefem.org.